■ ORIGINAL ARTICLE

Right atrial phasic function and outcome in patients with heart failure and reduced ejection fraction: Insights from speckle-tracking and three-dimensional echocardiography

Aura Vîjîiac[1, 2], Radu Vătășescu[1, 2], Sebastian Onciul[1, 2], Claudia Guzu[2], Violeta Verinceanu[2], Ioana Petre[1, 2], Silvia Deaconu[2], Alina Scărlătescu[2], Diana Zamfir[2], Alexandru Scafa-Udriște[1, 2], Maria Dorobanțu[1, 2]

[1]Department of Cardiology, "Carol Davila" University of Medicine and Pharmacy, Bucharest, Romania
[2]Department of Cardiology, Emergency Clinical Hospital, Bucharest, Romania

ABSTRACT

Background: Atrial phasic function can be assessed using speckle-tracking and three-dimensional (3D) echocardiography. The extent and role of right atrial (RA) dysfunction in left-sided heart failure (HF) is incompletely understood. We aimed to characterize RA phasic function in HF with reduced ejection fraction (HFrEF) and to assess its prognostic significance.

Methods: We prospectively enrolled 60 patients with HFrEF and 29 normal controls. RA phasic function was assessed using strain curves derived from speckle-tracking echocardiography and 3D volumetric analysis. Patients were followed for a composite endpoint of cardiac death or rehospitalization for HF.

Results: After a mean follow-up of 19 (9) months, 33 patients reached the primary endpoint. Patients with HFrEF and adverse outcomes showed an impairment of both reservoir, conduit, and booster pump RA function when compared to controls. After adjustment for age, left ventricular systolic and diastolic function, right ventricular systolic function and pulmonary artery pressure, RA maximal and minimal volumes, as well as passive emptying fraction, remained independent predictors of death or rehospitalization (hazard ratio [HR], 3.207; 95% confidence interval [CI], 1.288–7.984; *P* = 0.012; HR, 2.362, 95% CI, 1.004–5.552; *P* = 0.049; and HR, 2.367; 95% CI, 1.066–5.259; *P* = 0.034, respectively).

Conclusion: All three components of RA phasic function are impaired in left-sided HF. 3D RA maximal and minimal volumes, as well as 3D RA passive emptying fraction, are independent predictors of adverse outcomes in HFrEF.

Key words: right atrium, heart failure with reduced ejection fraction, atrial phasic function, atrial strain, 3D atrial volumes

INTRODUCTION

Both atria are highly dynamic chambers, with three mechanical functions which are related to the phases of the cardiac cycle: a reservoir function, serving as a storage for venous return during the ventricular systole; a conduit function, passively transferring the blood to the ventricle during the early ventricular diastole; and a booster pump function, actively forcing the blood into the ventricle during the late ventricular diastole [1]. Left atrial (LA) dysfunction is a well-established predictor of adverse outcomes in various clinical conditions [2–6], particularly in heart failure (HF) with either reduced or preserved ejection fraction (EF), and LA reservoir and contraction strain showed a good correlation with LA pressures [7]. However, the extent of right atrial (RA) dysfunction in HF and its prognostic significance remain to be clarified. Novel techniques such as three-dimensional (3D) and speckle-tracking echocardiography (STE) [8] allow a more refined evaluation of atrial phasic function.

WHAT'S NEW?

Right atrial geometry and function can be assessed with modern echocardiographic techniques such as speckle-tracking and three-dimensional (3D) echocardiography, but the role of this chamber in left-sided heart failure has been mostly neglected. In our study, we evaluated the morphology, function, and prognostic significance of the right atrium (RA) in patients with heart failure and reduced ejection fraction (HFrEF). We found that RA reservoir, conduit, and booster pump functions are all impaired in left-sided heart failure and that 3D RA maximal and minimal volumes, as well as 3D RA passive emptying fraction, are independent predictors of cardiac death and rehospitalization in HFrEF.

This study aimed to characterize the RA phasic function in HF with reduced EF (HFrEF), using 3D echocardiography and two-dimensional (2D) longitudinal strain derived from STE, and to assess the prognostic role of RA remodeling and mechanism in patients with HFrEF.

METHODS

Study population

We prospectively screened eighty-five consecutive outpatients with HFrEF who were referred to our echocardiography department between July 2018 and December 2018. The diagnostic of HFrEF [9] was based on the following criteria: symptoms and/or signs of HF and left ventricular (LV) EF <40% measured by the 2D Simpson biplane method. Exclusion criteria were atrial fibrillation or other significant arrhythmias which would have hampered 3D acquisitions (n = 9); a poor acoustic window, which would have made echocardiographic measurements unreliable (n = 7); inability to hold the breath (n = 3); the presence of comorbidities with life expectancy less than one year (n = 3); and significant respiratory diseases such as COPD (n = 2), and obstructive sleep apnea (n = 1). Sixty patients were thus eligible to form the final study population. They were clinically and hemodynamically stable, with no change in diuretic dose for at least 2 weeks before enrollment. Twenty-nine subjects with similar age and sex, referred for echocardiographic evaluation between July 2018 and December 2018, with no signs/ symptoms of HF, no structural heart disease, and normal left ventricular ejection fraction (LVEF) at echocardiography formed the control group. Recorded clinical data included cardiovascular risk factors, arterial blood pressure, and the New York Heart Association (NYHA) class, as well as brain natriuretic peptide (BNP) levels, when available. The study protocol complied with the Declaration of Helsinki, and it was approved by the ethics committee of our hospital; all participants provided written informed consent.

Echocardiography

An experienced sonographer performed 2D and 3D echocardiographic acquisitions according to current international recommendations [10], using a Vivid E9 (GE Vingmed, Horten, Norway) ultrasound machine equipped with a 2.5 MHz 2D matrix array transducer and a 4V probe.

Offline data analysis was done using dedicated software (EchoPAC BT 12).

RA transversal diameter and RA area were measured at end-systole in the apical 4-chamber view. For 2D RA strain, we selected the apical 4-chamber view in which the free wall of the RA was best visualized. We performed high frame rate acquisitions (50–70 frames per second), and we used vendor-specific software originally designed for the LV (EchoPAC — Q Analysis package). The endocardial border of the RA was manually traced, beginning and ending at the tricuspid annulus, and the width of the region of interest (ROI) was manually adjusted to include the whole endocardium, but not the pericardium, as recommended [11]. A visual revision was performed, and readjustments of the ROI were done when needed. The zero-strain reference point was set at the time of the QRS complex (end-diastole) [11]. The software automatically divided the RA wall into six segments and provided an averaged strain curve of these segments, which was used to measure the reservoir RA strain (RASr), measured as the maximal longitudinal displacement at end-systole (having a positive value), and the contraction RA strain (RASct), measured as the difference between strain at ventricular end-diastole and strain at the time of atrial systole (having a negative value, as recommended [11]) (Figure 1).

Similarly, we traced the right ventricular (RV) endocardial border to measure RV strain, while the software divided the RV free wall and the interventricular septum (IVS) into three segments each, providing a six-segment model. The global longitudinal strain of the RV (GLS-RV) was measured as the average of the six segmental values, and the longitudinal strain of the RV free wall (RVFW-LS) as the average of the three segmental values of the free wall. The severity of the tricuspid regurgitation (TR) was graded using qualitative Doppler criteria, such as color flow jet area and the shape and density of the TR jet envelope [12]. Pulmonary artery systolic pressure (PASP) was estimated using the sum of the peak TR gradient — obtained from the continuous-wave Doppler spectrum of the TR jet — and the estimated RA pressure, based on the inferior vena cava (IVC) diameter and respiratory changes [10].

For 3D RA volumes, we used six-beat full-volume acquisitions from the apical 4-chamber view, with electrocardiographic gating during breath holding and 8–22 frames per second. The pyramidal volume of the RA was displayed in
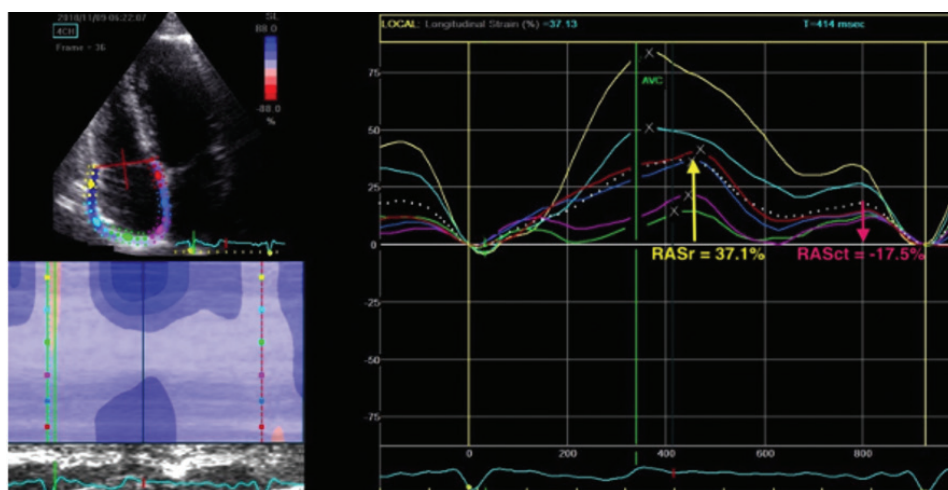
Figure 1. Measurement of RA strain using STE in the apical 4-chamber view. The six colored curves represent strain curves for six different segments of the RA. The dotted curve represents the average strain which was used to measure RAS_r (having a positive value) and RAS_{ct} (having a negative value)

Abbreviations: STE, speckle tracking echocardiography; other — see Table 1
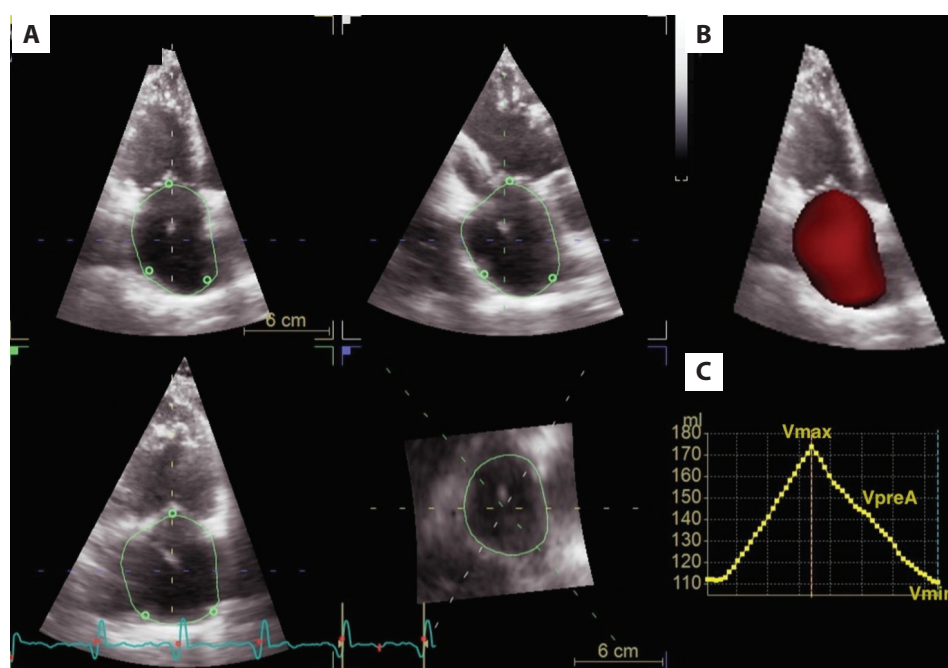

Figure 2. 3D assessment of the RA. Tracking of the RA border is manually readjusted in longitudinal and transverse views (**A**) to determine the 3D RA reconstruction superimposed on the greyscale 3D data set (**B**). The time-volume curve (**C**) depicts RA volume changes during the cardiac cycle and allows measurement of V_{max}, V_{preA}, and V_{min}

Abbreviations: see Table 1

three orthogonal long-axis and one short-axis plane. The RA plane was tilted and translated to have the long axis of the RA in the centerline, and manual landmarks were set in the apical views, two markings at the tricuspid annulus, and one marking at the base of the RA in each plane. The software automatically reconstructed the 3D endocardial surface of the RA — which was manually readjusted if needed — and provided the RA minimum volume (RAV_{min}), at ventricular end-diastole, RA preA volume (RAV_{preA}), at the peak of the P wave on ECG, and RA maximum volume (RAV_{max}), at ventricular end-systole (Figure 2), which were

all indexed for body surface area. From these volumes, we calculated:
- The total emptying volume (EV), as the difference between RAV_{max} and RAV_{min}, reflecting RA reservoir function;
- The passive EV, as the difference between RAV_{max} and RAV_{preA}, reflecting RA conduit function;
- The active EV, as the difference between RAV_{preA} and RAV_{min}, reflecting RA booster function;
- The corresponding emptying fractions (EmF): the total EmF = total EV/RAV_{max}, the passive EmF = passive EV/RAV_{max}, and the active EmF = active EV/ RAV_{preA}.

Table 1. Reproducibility of measurements for RA strain and volumes

Variable	Intraobserver ICC (95% CI)	Interobserver ICC (95% CI)
RAS_r	0.983 (0.933–0.996)	0.975 (0.900–0.994)
RAS_{ct}	0.881 (0.533–0.970)	0.816 (0.312–0.953)
RAV_{max}	0.969 (0.883–0.992)	0.962 (0.859–0.990)
RAV_{min}	0.974 (0.904–0.993)	0.951 (0.825–0.987)
RAV_{preA}	0.968 (0.755–0.993)	0.938 (0.781–0.983)

For abbreviations see text

Abbreviations: ICC, intraclass coefficients; RA, right atrial; RASr, reservoir RA strain; RASct, contraction RA strain; RAV_{min}, RA minimum volume; RAV_{preA}, RA_{preA} volume, RAV_{max}, RA maximum volume

We also measured another parameter of RA reservoir function, the 3D RA expansion index (RAEI), which represents the relative RA volume increase during the RA reservoir phase [13] and is calculated as $100 \times$ total EV/RAV_{min}, as previously described for the LA [14].

Reproducibility
To test the intraobserver reproducibility of RA strain, as well as 3D RA volumes, measurements were repeated two weeks apart in 10 randomly selected patients from the study group. To test the interobserver reproducibility, the same 10 patients were measured by a second researcher, blinded to the prior measurements. We then calculated the intraclass coefficients (ICC) in a two-way mixed-effects model. Reproducibility results are presented in Table 1.

Follow-up
Patients were prospectively followed to ascertain the occurrence of any major adverse cardiovascular event (MACE). For the current study, we used a primary composite endpoint of cardiac death and any rehospitalization for HF. Cardiac death was defined as either sudden death, death resulting from an acute coronary syndrome, fatal arrhythmia, or acute exacerbation of HF. Follow-up was conducted for 19 (9) months, through check-up visits, when applicable, or phone contact otherwise.

Statistical analysis
The Kolmogorov-Smirnov test was used to check the normality of distribution. Continuous data were reported as mean and standard deviation or as median and interquartile range, depending on the distribution. Categorical data were displayed as numbers and percentages. To compare patients' characteristics, we used test or Fisher's exact test for categorical variables and the one-way ANOVA or Kruskal-Wallis tests (as dictated by distribution), with a pairwise posthoc Tukey test for continuous variables. Correlations between continuous variables were assessed using Pearson's correlation coefficient.

To compare the accuracy of RA parameters to predict adverse outcomes, receiver operating characteristic (ROC) curves and the respective area under the curve (AUC) were used, while cut-off values were chosen based on the highest sum of sensitivity and specificity. We performed Cox proportional hazards regression to determine the prognostic value of these parameters. Results were reported as hazard ratios (HR) with 95% confidence intervals (CI). The multivariable model was constructed using age and well-established MACE predictors in left-sided heart failure, such as parameters of LV systolic and diastolic function, parameters of RV function, and PASP. Kaplan-Meier analysis was used for event-free survival and the log-rank test was used to compare survival curves. We used the SPSS version 20.0 statistical software package for all analyses. Statistical significance was defined as a two-tailed p-value <0.05.

RESULTS

Clinical characteristics
Mean age was 61 (14) years in the study group and 57 (9) years in the control group ($P = 0.10$), and in both groups, the majority were men (67% and 66%, respectively). Baseline demographic and clinical characteristics are summarized in Table 2. The etiology of HF in the study group was as follows: 28.3% ischemic heart disease, 25% valvular heart disease, 8.3% post-myocarditis, 13.3% familial cardiomyopathy, and 25% idiopathic dilated cardiomyopathy.

During a mean follow-up of 19 (9) months, 33 patients (55%) reached the primary endpoint: there were 7 cardiac deaths (11.7%) and 26 readmissions (43.3%) for exacerbation of HF. There were no significant differences in age, sex, or comorbidities between patients with and without MACE.

Echocardiographic findings
Echocardiographic measurements are summarized in Table 3. The extent of LV systolic dysfunction did not significantly differ between patients with MACE and without MACE. However, patients with MACE had significantly higher LA filling pressures and higher LA maximal volume than patients without MACE, reflecting a more severe diastolic dysfunction. Patients in our study group had RV involvement, as GLS-RV and RVFW-LS were both impaired in comparison with controls, and they were both significantly more impaired in patients with MACE. According to the normal cut-off of -20% for RVFW-LS recommended by guidelines [15], 66% of the patients in the study group had RV longitudinal dysfunction. While PASP was more elevated in the study group, it did not differ significantly between patients with and without MACE. More than mild TR was found in 13 (22%) patients from the study group, 2 of whom (3%) had severe TR.

Right atrial phasic function
In our study group, both RAS_r and RAS_{ct} were impaired while compared with controls; however, only RAS_r differed significantly between MACE and no MACE groups, being significantly more impaired in the former. 3D assessment of the RA showed significantly higher RA indexed volumes (maximal, minimal, and preA) in patients with adverse

Table 2. General characteristics of study participants

Variables	Control group (n = 29)	MACE (n = 33)	No MACE (n = 27)	P for all
Age, years, mean (SD)	57 (9)	61 (14)	60 (14)	0.32
Male sex, n (%)	19 (66)	23 (70)	17 (63)	0.86
Comorbidities				
Hypertension, n (%)	13 (45)	21 (64)	20 (74)	0.07
Diabetes mellitus, n (%)	3 (10)	7 (21)	4 (15)	0.50
Smoking, n (%)	15 (52)	10 (30)	18 (67)[c]	0.02
NYHA class				
Class I, n (%)	N/A	0 (0)	2 (7)	0.01
Class II, n (%)	N/A	10 (30)	17 (63)	
Class III, n (%)	N/A	19 (58)	7 (26)	
Class IV, n (%)	N/A	4 (12)	1 (4)	
Medication				
ACE-I/ARB/ARN-I, n (%)	8 (28)	32 (97)[a]	27 (100)[a]	<0.001
β-blockers, n (%)	13 (45)	32 (97)[a]	27 (100)[a]	<0.001
MRA, n (%)	0 (0)	31 (94)[a]	27 (100)[a]	<0.001
Loop diuretic, n (%)	1 (3)	27 (82)[a]	14 (52)[a, d]	<0.001
Aspirin, n (%)	13 (45)	20 (61)	21 (78)[b]	0.04
BNP levels, pg/ml, median (IQR)	88 (68–99)	703 (403–1000)[a]	378 (199–503)[b, d]	<0.001

Continuous data are expressed as mean (standard deviation [SD]) or median (interquartile range [IQR]). Categorical data are expressed as number (percentage)

[a]$P <0.001$ vs. control group. [b]$P <0.05$ vs. control group. [c]$P <0.01$ vs. MACE group. [d]$P <0.05$ vs. MACE group

Abbreviations: ACE-I, angiotensin-converting enzyme inhibitor; ARB, angiotensin receptor blocker; ARN-I, angiotensin receptor neprilysin inhibitor; BNP, brain natriuretic peptide; MACE, major adverse cardiac events; MRA, mineralocorticoid receptor antagonist; NYHA, New York Heart Association

Table 3. Echocardiographic findings

Variables	Control group (n=29)	MACE (n=33)	No MACE (n=27)	P for all
Left heart parameters				
LVEF, %	56 (4)	25 (7)[a]	27 (7)[a]	<0.001
Mitral E/A ratio	1.34 (0.30)	1.53 (0.72)	1.05 (0.90) *	0.03
Mitral E/E′ ratio	6 (5–8)	16 (11–20)[a]	11 (7–14)[a, d]	<0.001
LA maximal volume, ml	45 (39–54)	79 (67–117)[a]	59 (41–88)[d]	<0.001
Right heart parameters				
RV diameter, mm	34 (32–37)	37 (34–45)[b]	34 (31–37)[f]	0.006
GLS-RV, %	−21.3 (1.4)	−10.5 (4.7)[a]	−13.1 (4.6)[a, e]	<0.001
RVFW-LS, %	−28.7 (2.7)	−12.6 (10.3)[a]	−17.4 (7.4)[a, f]	<0.001
RA diameter, mm	34 (7)	42 (10)[b]	36 (7)[f]	<0.001
RA area, cm²	15 (13–17)	15 (14–23)	14 (12–16)	0.13
Tricuspid E/A ratio	1.07 (0.27)	1.37 (0.36)[b]	1.09 (0.38)[e]	<0.001
Tricuspid E/E′ ratio	6.2 (1.5)	6.3 (3.2)	5.1 (2.4)	0.16
RAS$_r$, %	29.0 (8.8)	15.6 (9.8)[a]	21.9 (11.9)[c, f]	<0.001
RAS$_{ct}$, %	−14.1 (5.6)	−8.8 (7.4)[c]	−12.1 (6.5)	0.006
3D RAV$_{max}$ index, ml/m²	18 (17–24)	27 (22–46)[a]	20 (17–33)[f]	0.002
3D RAV$_{min}$ index, ml/m²	9 (8–12)	17 (11–32)[a]	12 (8–16)[e]	<0.001
3D RAV$_{preA}$ index, ml/m²	14 (12–18)	22 (16–38)[a]	15 (13–22)[f]	<0.001
3D Total EV, ml	20 (7)	22 (13)	19 (10)	0.47
3D Total EmF, %	52 (49–56)	38 (26–45)[a]	43 (34–49)[a, f]	<0.001
3D Passive EV, ml	11 (9–15)	9 (6–13)	8 (6–13)	0.36
3D Passive EmF, %	28 (7)	18 (8)[a]	24 (9)[f]	<0.001
3D Active EV, ml	9 (7–11)	8 (5–14)	7 (4–12)	0.26
3D Active EmF, %	32 (8)	21 (11)[a]	24 (11)[b]	<0.001
3D RAEI	110 (22)	61 (29)[a]	79 (37)[a, f]	<0.001
More than mild TR, n (%)	2 (7)	10 (30)[c]	3 (11)	0.03
PASP, mm Hg	21 (19–24)	39 (28–51)[a]	34 (26–41)[a]	<0.001

Data are expressed as mean (standard deviation [SD]) or median (interquartile range [IQR])

[a]$P <0.001$ vs. control group. [b]$P <0.01$ vs. control group. [c]$P <0.05$ vs. control group. [d]$P <0.001$ vs. MACE group. [e]$P <0.01$ vs. MACE group. [f]$P <0.05$ vs. MACE group

Abbreviations: E/A, ratio between early mitral/tricuspid inflow velocity (E wave) and late velocity corresponding to atrial contraction (A wave) derived from pulsed-wave Doppler; E/E′, ratio between early mitral/tricuspid inflow velocity E derived from pulsed-wave Doppler and early mitral/tricuspid annulus velocity E′ derived from tissue Doppler imaging; EmF, emptying fractions; EV, emptying volume; PASP, pulmonary artery systolic pressure; RAEI, RA expansion index; TR, tricuspid regurgitation; other — see Table 1

Table 4. AUC and optimal cut-off value for RA functional parameters to identify patients with MACE

Parameter	AUC (95% CI)	P-value	Cut-off value	Sensitivity, %	Specificity, %
RAS$_r$	0.662 (0.522–0.803)	0.032	19.1%	75.8	63
RAS$_{ct}$	0.655 (0.515–0.795)	0.040	−9.3%	60.6	74.1
3D RAV$_{min}$ index	0.709 (0.578–0.840)	0.006	16 ml	63.6	77.8
3D RAV$_{max}$ index	0.686 (0.550–0.821)	0.014	22 ml	75.8	63
3D RAV$_{preA}$ index	0.700 (0.569–0.831)	0.008	19 ml	66.7	63
3D Total EV	0.571 (0.424–0.718)	0.345	14 ml	75.8	40.7
3D Total EmF	0.641 (0.500–0.782)	0.062	42%	72.7	55.6
3D Passive EV	0.538 (0.387–0.688)	0.619	9 ml	69.7	55.6
3D Passive EmF	0.684 (0.545–0.822)	0.015	18%	66.7	74.1
3D Active EV	0.599 (0.455–0.743)	0.189	6 ml	69.7	44.4
3D Active EmF	0.562 (0.415–0.709)	0.414	23%	66.7	48.1
3D RAEI	0.641 (0.500–0.782)	0.062	73	72.7	55.6

Abbreviations: AUC, area under the curve; see Tables 1, 2, and 3

Table 5. Cox regression analysis for parameters of RA phasic function as predictors of MACE

Variables	Unadjusted		Adjusted[a]	
	HR (95% CI)	P-value	HR (95% CI)	P-value
2D RAS$_r$	2.792 (1.255–6.213)	0.012	1.883 (0.787–4.506)	0.155
2D RAS$_{ct}$	2.475 (1.228–4.986)	0.011	1.980 (0.910–4.311)	0.085
3D RAV$_{max}$ index	3.544 (1.577–7.966)	0.002	3.207 (1.288–7.984)	0.012
3D RAV$_{min}$ index	3.188 (1.556–6.533)	0.002	2.362 (1.004–5.552)	0.049
3D RAV$_{preA}$ index	2.424 (1.164–5.048)	0.018	1.937 (0.828–4.534)	0.127
3D Total EV	1.836 (0.823–4.096)	0.138	1.655 (0.694–3.948)	0.256
3D Total EmF	2.124 (0.986–4.576)	0.055	1.686 (0.731–3.887)	0.220
3D Passive EV	2.036 (0.967–4.287)	0.061	2.040 (0.945–4.403)	0.069
3D Passive EmF	2.716 (1.311–5.625)	0.007	2.367 (1.066–5.259)	0.034
3D Active EV	1.659 (0.788–3.493)	0.182	1.300 (0.582–2.904)	0.522
3D Active EmF	1.404 (0.681–2.897)	0.358	1.554 (0.716–3.370)	0.265
3D RAEI	2.124 (0.986–4.576)	0.055	1.686 (0.731–3.887)	0.220

*Adjusted for age, LVEF, mitral E/E' ratio, RVFW-LS, and PASP

Abbreviations: see Tables 1, 2, and 3

outcomes, both in comparison to the control group and to the HF patients without MACE at follow-up. Patients with MACE had lower total EmF, lower passive EmF, and lower RAEI than both patients without MACE and controls, reflecting RA reservoir and conduit dysfunction in patients with adverse outcomes. Patients in the study group also had RA booster pump dysfunction (namely, lower active EmF) when compared with controls, but with no significant difference between patients with and without MACE.

RAS$_r$ showed a negative correlation, while RAS$_{ct}$ showed a positive correlation with GLS-RV (r = −0.53; P <0.001 and r = 0.35; P = 0.006, respectively) and PASP (r = −0.33; P = 0.01 and r = 0.38; P = 0.003, respectively). All three RA volumes had a modest positive correlation with PASP (r = 0.37; P = 0.004 for all), while RAV$_{min}$ and RAV$_{preA}$ were also weakly correlated to GLS-RV (r = 0.26; P = 0.040 and r = 0.25; P = 0.049, respectively). None of the RA phasic volumes or emptying fractions were correlated to PASP (P >0.05 for all). However, there was a modest negative correlation between GLS-RV and total EmF (r = −0.38; P = 0.002), passive EmF (r = −0.32; P = 0.01), active EmF (r = −0.26; P = 0.04), and RAEI (r = −0.39; P = 0.002). RA strain and volumes showed

no correlation with indices of RV diastolic function, but the tricuspid E/A ratio was weakly correlated with active EV (r = 0.31; P = 0.02), and the E/E' ratio was weakly correlated with total EmF (r = −0.31; P = 0.02), passive EmF (r = −0.26; P = 0.04), and RAEI (r = −0.27; P = 0.03).

Prognostic role of the right atrium
In ROC analysis, all three RA indexed volumes and passive EmF showed the best AUC, while cut-offs for event prediction and their corresponding sensitivity and specificity are shown in Table 4. RA volumetric and functional indices were tested using the Cox proportional hazards model for their ability to predict MACE. In univariable analysis (Table 5), RAS$_r$, RAS$_{ct}$, 3D indexed RAV$_{max}$, RAV$_{min}$, and RAV$_{preA}$, and passive EmF were significant predictors of adverse events (P <0.05 for all), reflecting that greater impairment of RA reservoir, conduit, or pump function determine an increased risk of adverse outcome. In unadjusted Kaplan-Meier analysis, the difference in event-free survival was greater when stratified by indexed RAV$_{max}$ and RAV$_{min}$ (Figure 3).

The multivariable model was constructed to be as simple as possible, to avoid overfitting while including
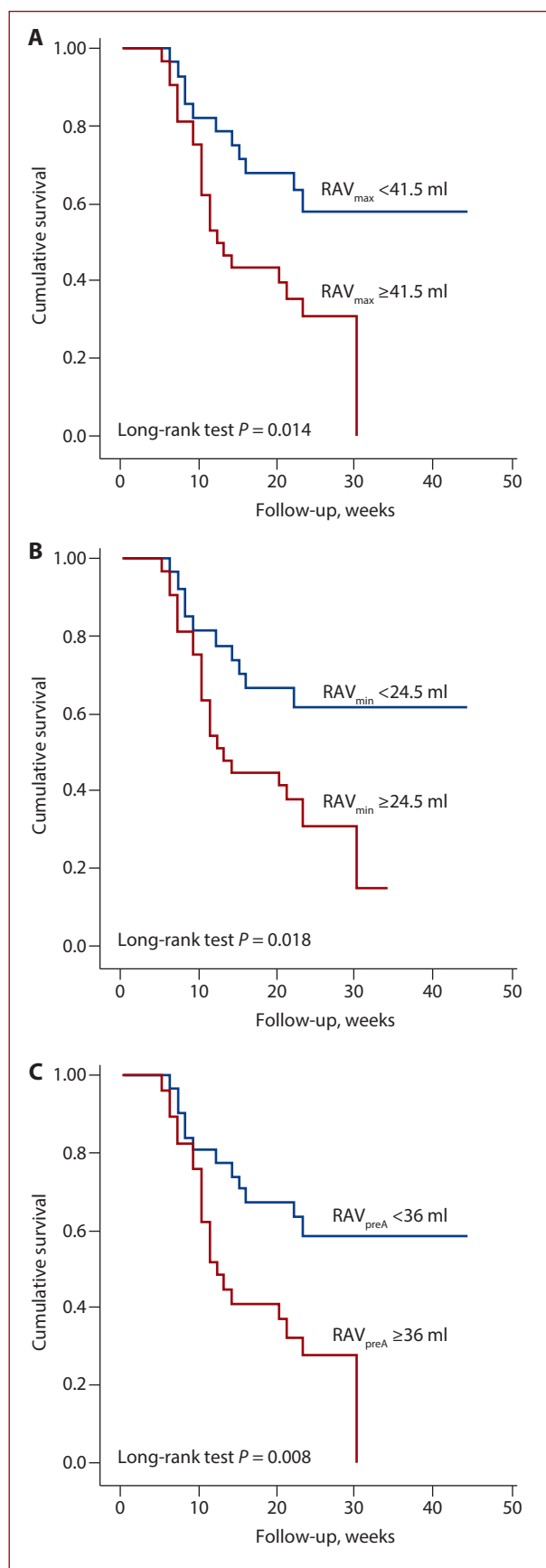
Figure 3. Kaplan-Meier survival curves stratified by the optimized cut-off value of $RAV_{max} > 41.5$ ml (**A**), $RAV_{min} > 24.5$ ml (**B**), and $RAV_{preA} > 36$ ml (**C**)

Abbreviations: see Table 1

established MACE predictors, such as age and parameters reflecting LV systolic and diastolic function, RV function, and the degree of pulmonary hypertension. In multivariable analysis, passive EmF, indexed RAV_{max}, and indexed RAV_{min} remained independent predictors of MACE after adjustment for age, LVEF, mitral E/E′ ratio, RVFW-LS, and PASP (Table 5). An indexed RAV_{max} larger than 22 ml was associated with a more than 3-fold risk for MACE, while an indexed RAV_{min} larger than 16 ml and a passive EmF less than 18% determined a more than 2-fold risk for events. BNP levels were not included in the multivariable analysis since they were not available for all patients. The degree of TR was not included in the model because it was not a significant predictor of adverse outcomes in univariable analysis ($P = 0.06$).

DISCUSSION

In this study, we assessed the RA volumes and phasic function among patients with HFrEF and evaluated the prognostic role of RA dysfunction in these patients. Our findings can be summarized as follows: (1) all RA volumes were significantly larger in patients with HFrEF and MACE when compared with both normal subjects and with HF patients without MACE; (2) patients with HFrEF and MACE have impaired RA reservoir (RAS_r, total EmF, and RAEI), conduit (passive EmF) and booster pump function (RAS_{ct} and active EmF) in comparison to controls; (3) indexed RAV_{max}, RAV_{min}, and passive EmF are independent predictors of outcome in HFrEF after adjustment for age, LVEF, mitral E/E′ ratio, PASP, and RVFW-LS.

While the prognostic role of RV dysfunction [16, 17] and LA phasic function [6] in HFrEF are well recognized, the role of the RA in diseases of the left heart is frequently overlooked. Conventional evaluation of the RA includes measurement of RA diameter and area, while 2D volumetric assessment is not routinely recommended [15]. Since RA remodeling is often asymmetrical, 3D measurements can assess the atrial size more accurately than 2D echocardiography [18]. STE and 3D echocardiography are useful tools for the characterization of RA phasic function and remodeling, and both RA reservoir strain [19] and 3D RA volumes [20] were found to be good diagnostic tools for identifying elevated RA pressure. While RA function has been studied in pulmonary arterial hypertension using innovative echocardiographic techniques [21, 22] and cardiac magnetic resonance (CMR) [23, 24], data regarding the phasic function of the RA in left-sided HF are scarce.

Normal reference values for RA strain indices and 3D volumes have been previously defined [18, 25]; however, this is the first study so far that assesses the RA size and function with both STE and 3D echocardiography in patients with HFrEF. In our study, all 3D RA volumes were larger, and all 3D emptying fractions, as well as RA strain indices, were lower in patients with MACE than in normal controls. Previous research reported altered RA reservoir strain in HF patients [26], while Jain et al. found in their

CMR study that HFrEF patients have an alteration of both RA reservoir and conduit function [27]. To our knowledge, our study is the first one to report impairment of all three components of RA phasic function in patients with HFrEF.

The RA maximal volume index (RAVI) assessed with 2D echocardiography was previously found to be an independent predictor of death, heart transplantation, and/or HF rehospitalization in patients with chronic systolic HF [28]. Similar results were reported by Proplesch et al. [29], who found that RAVI, but also RA total EmF, were predictors of death or 12-month rehospitalization in a cohort of patients with HF. Furthermore, a CMR study also found that RAVI is an independent mortality predictor in HFrEF [30], providing an additional contribution to the mortality risk stratification. Consistent with these previous findings, our study is the first, so far, to report the independent predictive value of both 3D indexed RAV_{max} and RAV_{min} in patients with HFrEF. An enlarged RAV_{max} was associated with a more than 3-fold, while an enlarged RAV_{min} was associated with a more than 2-fold hazard of adverse events in patients with HFrEF. We also found that a passive RA EmF < 18% determined a more than 2-fold hazard of MACE, reflecting the importance of RA conduit dysfunction in determining adverse outcomes. As it has been previously stated [31], atrial reservoir and pump functions have a greater contribution to ventricular stroke volume in the initial stages of cardiac disease, while conduit function becomes most important in advanced stages when ventricular diastolic pressure rises and the role of the other two phasic functions diminishes.

The RA and RV have a complex interplay throughout the whole cardiac cycle. On the one hand, the RA is more than just a blood receptacle, acting as a dynamic modulator of RV performance by redistributing RV filling and ejection force among reservoir, conduit, and booster functions. The atrial compliance directly influences the filling of the ventricle, and atrial phasic dysfunction will impair ventricular performance and reduce cardiac output [32]. On the other hand, the RV is subject to increased afterload in left-sided HF, which will determine RV remodeling and hypertrophy, increase RV pressure, and result in subsequent elevation of RA pressure. However, in our study, RA volumes and passive EmF remained independent outcome predictors even after adjusting for PASP and RV systolic function, which reinforces the idea that the RA is not a passive transit chamber but an active cavity allowing dynamic energy transfer to the ventricle [33], modulating the ventricular performance and having prognostic implications. While the severity of functional TR is highly dependent on loading conditions, the degree of TR did not predict events in our study. A probable explanation is that our cohort included stable outpatients, the majority with mild TR, with stable doses of diuretics. This suggests that the RA functional impairment and its predictive role in our study are related to an intrinsic alteration of the RA mechanics rather than to the degree of functional TR.

While some authors suggest that RA size is merely a surrogate of RV diastolic function [34], we found no correlations between RA volumes and tricuspid E/A and E/E' ratios in our study. A possible explanation for this is that RV diastolic function and RV filling pressure are related not only to RA size but also to its stiffness and contractility. This implies that RA mechanics has an independent pathophysiological role in left-sided HF, an idea that has been previously suggested [35]. Our results highlight that RA assessment in left-sided HF should not be neglected and that measuring just the currently recommended end-systolic dimensions might not be enough.

Study limitations

This study should be interpreted in the context of several limitations. While it has the advantage of being a prospective study, its main limitation is the small sample size and the relatively short follow-up period. Second, we excluded patients with a poor acoustic window, which brings a potential selection bias. More importantly, we did not include patients with atrial fibrillation to avoid stitch artifacts in 3D echocardiography, and since atrial fibrillation determines changes in atrial size and function, it is uncertain whether our results apply to patients with HFrEF and atrial arrhythmias. Last but not least, for RA assessment we used vendor-specific software that was initially designed for the LV; hence, the cut-off values we reported in ROC analysis might not apply to other software.

CONCLUSION

Our study is the first one to report a comprehensive assessment of phasic RA function, using STE and 3D echocardiography, in patients with HFrEF, including evaluation of its prognostic value. We found that all three RA volumes and all three components of RA mechanics were impaired in patients with HFrEF and adverse outcomes. Moreover, we found that 3D RA maximal and minimal volumes, as well as 3D passive EmF, were independent predictors of major adverse events, irrespective of well-established demographic and echocardiographic risk factors. Further studies are needed to evaluate if RA phasic function retains its prognostic value in long-term follow-up. However, these results reinforce the idea that the RA is not just a passive transit chamber, and its evaluation should not be overlooked in patients with left-sided HF.

Article information

REFERENCES

1. Blume GG, Mcleod CJ, Barnes ME, et al. Left atrial function: physiology, assessment, and clinical implications. Eur J Echocardiogr. 2011; 12(6): 421–430, doi: 10.1093/ejechocard/jeq175, indexed in Pubmed: 21565866.

2. Sanchis L, Gabrielli L, Andrea R, et al. Left atrial dysfunction relates to symptom onset in patients with heart failure and preserved left ventricular ejection fraction. Eur Heart J Cardiovasc Imaging. 2015; 16(1): 62–67, doi: 10.1093/ehjci/jeu165, indexed in Pubmed: 25187609.

3. Santos ABS, Roca GQ, Claggett B, et al. Prognostic relevance of left atrial dysfunction in heart failure with preserved ejection fraction. Circ Heart Fail. 2016; 9(4): e002763, doi: 10.1161/CIRCHEARTFAILURE.115.002763, indexed in Pubmed: 27056882.

4. Santos ABS, Kraigher-Krainer E, Gupta DK, et al. Impaired left atrial function in heart failure with preserved ejection fraction. Eur J Heart Fail. 2014; 16(10): 1096–1103, doi: 10.1002/ejhf.147, indexed in Pubmed: 25138249.

5. Malagoli A, Rossi L, Bursi F, et al. Left atrial function predicts cardiovascular events in patients with chronic heart failure with reduced ejection fraction. J Am Soc Echocardiogr. 2019; 32(2): 248–256, doi: 10.1016/j.echo.2018.08.012, indexed in Pubmed: 30316541.

6. Rossi A, Carluccio E, Cameli M, et al. Left atrial reservoir function and outcome in heart failure with reduced ejection fraction. Circ Cardiovasc Imaging. 2018; 11(11): e007696–4759, doi: 10.1161/CIRCIMAGING.118.007696, indexed in Pubmed: 30571318.

7. Uziębło-Życzkowska B, Krzesiński P, Jurek A, et al. Correlations between left atrial strain and left atrial pressures values in patients undergoing atrial fibrillation ablation. Kardiol Pol. 2021; 79(11): 1223–1230, doi: 10.33963/KP.a2021.0113, indexed in Pubmed: 34599496.

8. Kupczyńska K, Mandoli GE, Cameli M, et al. Left atrial strain — a current clinical perspective. Kardiol Pol. 2021; 79(9): 955–964, doi: 10.33963/KP.a2021.0105, indexed in Pubmed: 34599503.

9. McDonagh TA, Metra M, Adamo M, et al. 2021 ESC Guidelines for the diagnosis and treatment of acute and chronic heart failure. Eur Heart J. 2021; 42(36): 3599–3726, doi: 10.1093/eurheartj/ehab368, indexed in Pubmed: 34447992.

10. Mitchell C, Rahko PS, Blauwet LA, et al. Guidelines for Performing a Comprehensive Transthoracic Echocardiographic Examination in Adults: Recommendations from the American Society of Echocardiography. J Am Soc Echocardiogr. 2019; 32(1): 1–64, doi: 10.1016/j.echo.2018.06.004, indexed in Pubmed: 30282592.

11. Badano LP, Kolias TJ, Muraru D, et al. Standardization of left atrial, right ventricular, and right atrial deformation imaging using two-dimensional speckle tracking echocardiography: a consensus document of the EACVI/ASE/Industry Task Force to standardize deformation imaging. Eur Heart J Cardiovasc Imaging. 2018; 19(6): 591–600, doi: 10.1093/ehjci/jey042, indexed in Pubmed: 29596561.

12. Zoghbi WA, Adams D, Bonow RO, et al. Recommendations for Noninvasive Evaluation of Native Valvular Regurgitation: A Report from the American Society of Echocardiography Developed in Collaboration with the Society for Cardiovascular Magnetic Resonance. J Am Soc Echocardiogr. 2017; 30(4): 303–371, doi: 10.1016/j.echo.2017.01.007, indexed in Pubmed: 28314623.

13. Genovese D, Muraru D, Marra MP, et al. Left atrial expansion index for noninvasive estimation of pulmonary capillary wedge pressure: a cardiac catheterization validation study. J Am Soc Echocardiogr. 2021; 34(12): 1242–1252, doi: 10.1016/j.echo.2021.07.009, indexed in Pubmed: 34311063.

14. Hsiao SH, Chiou KR. Left atrial expansion index predicts all-cause mortality and heart failure admissions in dyspnoea. Eur J Heart Fail. 2013; 15(11): 1245–1252, doi: 10.1093/eurjhf/hft087, indexed in Pubmed: 23703107.

15. Lang R, Badano L, Mor-Avi V, et al. Recommendations for Cardiac Chamber Quantification by Echocardiography in Adults: An Update from the American Society of Echocardiography and the European Association of Cardiovascular Imaging. Eur Heart J Cardiovasc Imaging. 2015; 16(3): 233–271, doi: 10.1093/ehjci/jev014, indexed in Pubmed: 25712077.

16. Adir Y, Guazzi M, Offer A, et al. all investigators. Different correlates but similar prognostic implications for right ventricular dysfunction in heart failure patients with reduced or preserved ejection fraction. Eur J Heart Fail. 2017; 19(7): 873–879, doi: 10.1002/ejhf.664, indexed in Pubmed: 27860029.

17. Vijiiac A, Onciul S, Guzu C, et al. The prognostic value of right ventricular longitudinal strain and 3D ejection fraction in patients with dilated cardiomyopathy. Int J Cardiovasc Imaging. 2021; 37(11): 3233–3244, doi: 10.1007/s10554-021-02322-z, indexed in Pubmed: 34165699.

18. Peluso D, Badano LP, Muraru D, et al. Right atrial size and function assessed with three-dimensional and speckle-tracking echocardiography in 200 healthy volunteers. Eur Heart J Cardiovasc Imaging. 2013; 14(11): 1106–1114, doi: 10.1093/ehjci/jet024, indexed in Pubmed: 23423966.

19. Miah N, Faxén UL, Lund LH, et al. Diagnostic utility of right atrial reservoir strain to identify elevated right atrial pressure in heart failure. Int J Cardiol. 2021; 324: 227–232, doi: 10.1016/j.ijcard.2020.09.008, indexed in Pubmed: 32941871.

20. Ostenfeld E, Werther-Evaldsson A, Engblom H, et al. Discriminatory ability of right atrial volumes with two- and three-dimensional echocardiography to detect elevated right atrial pressure in pulmonary hypertension. Clin Physiol Funct Imaging. 2018; 38(2): 192–199, doi: 10.1111/cpf.12398, indexed in Pubmed: 27925364.

21. Hasselberg NE, Kagiyama N, Soyama Y, et al. The prognostic value of right atrial strain imaging in patients with precapillary pulmonary hypertension. J Am Soc Echocardiogr. 2021; 34(8): 851–861.e1, doi: 10.1016/j.echo.2021.03.007, indexed in Pubmed: 33774108.

22. Querejeta Roca G, Campbell P, Claggett B, et al. Right atrial function in pulmonary arterial hypertension. Circ Cardiovasc Imaging. 2015; 8(11): 1–8, doi: 10.1161/CIRCIMAGING.115.003521, indexed in Pubmed: 26514759.

23. Bredfelt A, Rådegran G, Hesselstrand R, et al. Increased right atrial volume measured with cardiac magnetic resonance is associated with worse clinical outcome in patients with pre-capillary pulmonary hypertension. ESC Heart Fail. 2018; 5(5): 864–875, doi: 10.1002/ehf2.12304, indexed in Pubmed: 29916558.

24. Sato T, Tsujino I, Ohira H, et al. Right atrial volume and reservoir function are novel independent predictors of clinical worsening in patients with pulmonary hypertension. J Heart Lung Transplant. 2015; 34(3): 414–423, doi: 10.1016/j.healun.2015.01.984, indexed in Pubmed: 25813768.

25. Soulat-Dufour L, Addetia K, Miyoshi T, et al. Normal Values of Right Atrial Size and Function According to Age, Sex, and Ethnicity: Results of the World Alliance Societies of Echocardiography Study. J Am Soc Echocardiogr. 2021; 34(3): 286–300, doi: 10.1016/j.echo.2020.11.004, indexed in Pubmed: 33212183.

26. Ojaghi Haghighi Z, Naderi N, Amin A, et al. Quantitative assessment of right atrial function by strain and strain rate imaging in patients with heart failure. Acta Cardiol. 2011; 66(6): 737–742, doi: 10.1080/ac.66.6.2136957, indexed in Pubmed: 22299384.

27. Jain S, Kuriakose D, Edelstein I, et al. Right Atrial Phasic Function in Heart Failure With Preserved and Reduced Ejection Fraction. JACC Cardiovasc Imaging. 2019; 12(8 Pt 1): 1460–1470, doi: 10.1016/j.jcmg.2018.08.020, indexed in Pubmed: 30343071.

28. Sallach JA, Tang WH, Borowski AG, et al. Right atrial volume index in chronic systolic heart failure and prognosis. JACC Cardiovasc Imaging. 2009; 2(5): 527–534, doi: 10.1016/j.jcmg.2009.01.012, indexed in Pubmed: 19442936.

29. Proplesch M, Merz AA, Claggett BL, et al. Right atrial structure and function in patients with hypertension and with chronic heart failure. Echocardiography. 2018; 35(7): 905–914, doi: 10.1111/echo.13876, indexed in Pubmed: 29600555.

30. Ivanov A, Mohamed A, Asfour A, et al. Right atrial volume by cardiovascular magnetic resonance predicts mortality in patients with heart failure with reduced ejection fraction. PLoS One. 2017; 12(4): e0173245, doi: 10.1371/journal.pone.0173245, indexed in Pubmed: 28369148.

31. Nappo R, Degiovanni A, Bolzani V, et al. Quantitative assessment of atrial conduit function: a new index of diastolic dysfunction. Clin Res Cardiol. 2016; 105(1): 17–28, doi: 10.1007/s00392-015-0882-8, indexed in Pubmed: 26123829.

32. Gaynor SL, Maniar HS, Prasad SM, et al. Reservoir and conduit function of right atrium: impact on right ventricular filling and cardiac output.

Am J Physiol Heart Circ Physiol. 2005; 288(5): H2140–H2145, doi: 10.1152/ajpheart.00566.2004, indexed in Pubmed: 15591102.

33. Marino PN, Degiovanni A, Zanaboni J. Complex interaction between the atrium and the ventricular filling process: the role of conduit. Open Heart. 2019; 6(2): e001042, doi: 10.1136/openhrt-2019-001042, indexed in Pubmed: 31673383.

34. Vakilian F, Tavallaie A, Alimi H, et al. Right atrial strain in the assessment of right heart mechanics in patients with heart failure with reduced ejection fraction. J Cardiovasc Imaging. 2021; 29(2): 135–143, doi: 10.4250/jcvi.2020.0092, indexed in Pubmed: 33605100.

35. von Roeder M, Kowallick JT, Rommel KP, et al. Right atrial-right ventricular coupling in heart failure with preserved ejection fraction. Clin Res Cardiol. 2020; 109(1): 54–66, doi: 10.1007/s00392-019-01484-0, indexed in Pubmed: 31053957.